
Molecular Crystals and Liquid Crystals

Publication details, including instructions for authors and subscription information:
http://www.tandfonline.com/loi/gmcl20

# The Orientation of the Principal Axes of the Electron Dipolar Interaction Tensor in Triplet State C 60 Monoadducts

Stefano Ceola [a] , Carlo Corvaja [a] & Lorenzo Franco [a]

[a] Department of Physical Chemistry, University of Padova, via Loredan 2, Padova, 35131, Italy

Version of record first published: 18 Oct 2010

To cite this article: Stefano Ceola, Carlo Corvaja & Lorenzo Franco (2003): The Orientation of the Principal Axes of the Electron Dipolar Interaction Tensor in Triplet State C 60 Monoadducts, Molecular Crystals and Liquid Crystals, 394:1, 31-43

To link to this article: http://dx.doi.org/10.1080/15421400390193657

*Mol. Cryst. Liq. Cryst.*, Vol. 394, pp. 31–43, 2003

ISSN 1542-1406 print/1563-5287 online
DOI: 10.1080/15421400390193666

Taylor & Francis
Taylor & Francis Group

# THE ORIENTATION OF THE PRINCIPAL AXES OF THE ELECTRON DIPOLAR INTERACTION TENSOR IN TRIPLET STATE $C_{60}$ MONOADDUCTS

*Stefano Ceola, Carlo Corvaja, and Lorenzo Franco*
*Department of Physical Chemistry, University of Padova, via Loredan 2, 35131 Padova Italy*



*The time resolved EPR spectra of a fullerene monoadduct triplet state has been studied in nematic phase of E7. The EPR lineshape has been explained with a motionally averaged, preferentially oriented, triplet spectrum. From the knowledge of the order parameters of the $C_{60}$ adduct, obtained from the analysis of EPR spectra of a very similar $C_{60}$-nitroxide derivative dissolved in the same nematic solvent, it was possible to determine that the X principal axis of the triplet state dipolar tensor is parallel to the $C_2$ symmetry axis of the $C_{60}$ monoadduct.*

*Keywords*: fullerene derivatives; triplet state; EPR

## INTRODUCTION

The $C_{60}$ excited triplet state has been extensively studied in liquid solution, in single crystals [1], in glassy matrices [2] and dispersed in polymers [3]. In the ground state, $C_{60}$ is a highly symmetric molecule belonging to the symmetry group $I_h$. On the contrary, the symmetry in the excited triplet state is much lower, as shown by the EPR spectrum, characterised by non-vanishing zero field splitting (ZFS) parameters D and E, which reflect the magnetic dipolar interaction between the unpaired electron spins. Jahn-Teller effect which stabilises a distorted structure is the cause of symmetry lowering. Several distorted structures are possible, with very little energy separation [4] and in solution their interconversion averages very efficiently the ZFS interaction, giving an unusually narrow EPR line [5]. In fact the distortion can occur along different axes and transitions among different structures correspond to a pseudo-rotation of the molecule with respect to

This work was supported by CNR (legge 95/95) and by MURST (Contract Prot. MM03198284). We are grateful to Dr. G. Zordan (Organic Chemistry Department – University of Padova) who provided us with the samples of fullerene derivatives.

the Zeeman magnetic field direction. The EPR spectrum recorded in glassy matrices indicates a distortion with rombic symmetry, with $E \neq 0$. Such distortion is often not considered in calculations and the most significant distortion is considered to occur along one of the fivefold symmetry axes of the ground state $C_{60}$.

Modified fullerenes, such as fulleropyrrolidines [6] and methanofullerenes [7], have a low symmetry ($C_{2v}$, $C_s$ or lower) already in the ground state and Jahn-Teller effect is not operative. Moreover, as long as monoadducts are concerned, the ZFS parameters depend very little on the particular addend. It is surprising that D and E values for $C_{60}$ monoadducts are very similar to those of pristine $C_{60}$, indicating a similar unpaired electron distribution.

No information is available so far regarding the orientation of the principal axes of ZFS interaction with respect to the molecular axes. The maximum information at this regard consists in the fact that for $C_{2v}$ symmetrical derivatives, one axis should coincide with the twofold symmetry axis, and the others should be perpendicular to the first one and lying in the symmetry planes. In any case, it is not possible to assign them to the individual principal values, in particular is not possible to know a priori which direction corresponds to which principal value.

In a recent paper, a fulleropyrrolidine covalently linked to a stable nitroxide radical was considered [8]. When photoexcited by a laser light pulse, that derivative (3,4-fulleropyrrolidine-2-spiro-4′-[2′, 2′, 6′, 6′-tetramethyl] piperidine-1′-oxyl), gave rise to a transient EPR spectrum due to the excited quartet state, formed by the interaction of the radical unpaired electron with the triplet excited fullerene moiety. The quartet ZFS tensor was calculated considering contributions from the electron dipolar interaction within the fullerene triplet, and from the radical-triplet dipolar interaction. The calculated EPR spectra corresponded with the experimental ones assuming the triplet dipolar tensor oriented along one of the $C_5$ axes of the $C_{60}$ moiety, disregarding the local symmetry imposed by the position of addition. The deviation from the local $C_{2v}$ symmetry could be due to the low symmetry of the $C_{60}$ addend and to the interaction between the nitroxide electron density and the fullerene triplet electron density.

We consider the problem of identifying the orientation of the principal axes of dipolar interaction in the triplet state of $C_{60}$ monoadducts, with a derivative with higher symmetry and exploiting the method of partially orienting the molecules in liquid crystal solvents. The molecular structure of the adduct is shown in chart 1, together with that of a radical adduct.

Derivative **2** is a stable nitroxide free radical whose EPR spectrum is characterised by anisotropic g and $^{14}N$ hyperfine coupling tensors. This was used as reference, because the variation of its spectrum on going from the isotropic to the nematic phase allowed to obtain the ordering matrix, which

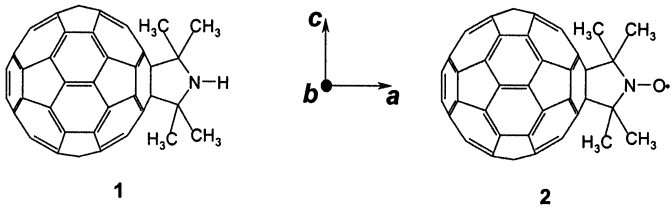


**CHART 1** Compounds studied in this work. The molecular axes system is defined choosing the *a* direction as going from the centre of the fullerene unit to the N atom (the local $C_2$ symmetry axis) and the *c* axis as parallel to the 6,6′ bond of the addition position to the fullerene.

is assumed to be the same for **1**, which has a very similar symmetric geometry. The time resolved EPR spectrum of photoexcited triplet state of **1** in nematic solution was interpreted on the basis of different choices for the assignment of the principal direction of the dipolar tensor. It turned out that the agreement with experimental spectra is obtained only with one out of the three different possibilities.

## EXPERIMENTAL

Compound **1** (3,4-fullero-[2, 2, 5, 5,-tetramethyl]-pyrrolidine) and compound **2** (3,4-fullero-[2, 2, 5, 5,-tetramethyl]-pyrrolidine-1-oxyl) were prepared following the synthesis reported in literature [6]. The samples for the EPR measurements were prepared dissolving **1** or **2** in E7 liquid crystal (Merck) with a concentration of about $10^{-3}$ M. A small amount (0.2 ml) of the solutions was inserted into EPR quartz tubes (3 mm i.d.). The solutions in the tubes were degassed with repeated freeze-pump-thaw cycles and then the tubes were sealed off under vacuum.

TR-EPR measurements were performed by irradiating with light pulses the sample placed inside the microwave cavity of a X-band EPR spectrometer (Bruker ER200) and recording the transient signal at each magnetic field positions. For the measurement at different temperatures a nitrogen-flow variable temperature system (Bruker ER4112VT) was used. A frequency-doubled pulsed Nd:YAG laser (Quantel Brilliant) was used as source of visible light ($\lambda = 532$ nm, pulse duration = 4 ns, energy per pulse 10 mJ). The TR-EPR signal evoked by the light pulse was amplified by a wide band preamplifier (bandwidth 20 Hz–6.5 MHz) and recorded by a digital oscilloscope (LeCroy 344LT). No field modulation was used, and the TR-EPR spectra represent true absorption or emission. In order to increase the signal to noise ratio, up to 200 transient signals were averaged for each magnetic field value.

## EPR of Triplet States

The triplet state spin Hamiltonian consists of the Zeeman interaction term and of the electron dipolar term. It is:

$$\mathrm{H} = \mathrm{g}\beta \boldsymbol{S}\boldsymbol{B} + \boldsymbol{S}\mathbf{D}\boldsymbol{S} \tag{1}$$

where $\boldsymbol{S}$ is the total spin operator, $\boldsymbol{B}$ is the magnetic field vector, $\mathbf{D}$ is the dipolar interaction tensor. The Hamiltonian is usually written in terms of two parameters D and E which are combination of the traceless dipolar tensor $\mathbf{D}$ eigenvalues ($\mathrm{D_{XX}}$, $\mathrm{D_{YY}}$, $\mathrm{D_{ZZ}}$).

$$\mathrm{D} = -\frac{3}{2}\mathrm{D_{ZZ}} \tag{2a}$$

$$\mathrm{E} = \frac{1}{2}(\mathrm{D_{YY}} - \mathrm{D_{XX}}) \tag{2b}$$

$$\mathrm{H} = \mathrm{g}\beta \boldsymbol{S}\boldsymbol{B} + \mathrm{D}S_Z^2 + \mathrm{E}(S_X^2 + S_Y^2) \tag{3}$$

where X, Y, Z are the principal directions of the ZFS interaction tensor. The eigenfunctions of H for $\boldsymbol{B} = 0$ are indicated by $|\mathrm{T_X}>, |\mathrm{T_Y}>$ and $|\mathrm{T_Z}>$. These substates are populated by ISC from the first excited singlet at different rates $\mathrm{k_X}$, $\mathrm{k_Y}$ and $\mathrm{k_Z}$, because, due to their different symmetry, spin-orbit interaction contaminates them with different amounts of singlet component.

In the presence of magnetic field, the triplet spin wave functions are a linear combination of the $|\mathrm{T_X}>, |\mathrm{T_Y}>$ and $|\mathrm{T_Z}>$ functions with coefficients which depend on the magnitude of $\boldsymbol{B}$ and on its orientation with respect to the ZFS tensor principal axes. The triplet spin functions in high magnetic field ($\boldsymbol{B} \gg$ D, E) are indicated by $|-1>, |0>$ and $|1>$. Their populating rates are linear combinations of $\mathrm{k_X}$, $\mathrm{k_Y}$ and $\mathrm{k_Z}$ with coefficients which depend on the orientation of $\boldsymbol{B}$.

$$\mathrm{k_r} = \sum\nolimits_{v} \mathrm{c}_v(\boldsymbol{\Omega})\mathrm{k}_v \tag{4}$$

where $\boldsymbol{\Omega}$ represents the orientation, $\mathrm{r} = -1, 0, 1$ and $v = \mathrm{X, Y, Z}$

The high field EPR spectrum of a triplet state molecule consists of the two $|-1> \Leftrightarrow |0>$ and $|0> \Leftrightarrow |1>$ allowed transitions, whose separation is a function of the ZFS parameters D and E and of the orientation of $\boldsymbol{B}$ with respect to X, Y and Z axes. If the spectrum is recorded just after a laser light pulse, before the triplet system reaches thermal equilibrium, the two transitions have the same absolute intensity, but they have opposite polarisation: one is in enhanced absorption and the second is in emission. EPR measurements performed on single crystals would allow to assign the ZFS parameters to orientations relative to crystal axes and to a molecular frame, if the crystal structure is known. Growing single crystals of fullerene

derivatives, suitable for EPR work, is a very difficult task. Moreover, in order to avoid intermolecular interactions, which possibly mediate the anisotropy, single crystals with the fullerene derivative diluted in a suitable host should be prepared, which adds to the difficulty. Therefore, in order to measure the ZFS parameters, one should rely on spectra of powder samples or glassy matrices, where all molecular orientations are present.

The EPR spectrum of a randomly oriented collection of triplet state molecules is the superposition of the pairs of lines corresponding to each molecular orientation. The overall shape depends on the ZFS parameters and on the zero field populating rates $k_X$, $k_Y$ and $k_Z$. With randomly oriented samples, no information could be obtained on the orientation of the principal axes with respect to the molecular axes.

In isotropic liquid solution, the rapid tumbling motion of the molecules averages to zero the anisotropy of the ZFS interaction, the $|-1> \Leftrightarrow |0>$ and $|0> \Leftrightarrow |1>$ transitions become degenerate and a single line is recorded. Its intensity is usually small because the spin polarisation vanishes, being the sum of opposite contributions.

In anisotropic solvents as liquid crystals, each molecule experiences all orientations but with differing probabilities. For fast molecular motion, the ZFS tensor is averaged over the orientation distribution, giving an effective ZFS tensor having axial symmetry around the liquid crystal director. The effective ZFS parameter ($D_{eff}$) is obtained from the ordering matrix **S** and the ZFS tensor **D**. Indicating by $\theta_i$ the angle between the principal axis i (i = X, Y, Z) and the director, **S** is defined by [9]:

$$S_{i,j} = \frac{1}{2}\langle 3(\cos\vartheta_i \cdot \cos\vartheta_j) - \delta_{ij}\rangle \tag{5}$$

The director of nematic liquid crystals is oriented by a magnetic field and the EPR spectrum of a triplet state molecule dissolved in these solvents consists of two lines whose separation is $2*D_{eff}$.

$$D_{eff} = -\mathrm{Tr}[\mathbf{S}\cdot\mathbf{D}] \tag{6}$$

This parameter depends on the temperature because of the temperature variation of the ordering matrix **S**.

The shape of the spectrum of photoexcited triplet states depends on the relative populations of the triplet sublevels $P_{-1}$, $P_0$, $P_1$, which at short delay time after a laser pulse are proportional to the populating rates $k_r$. It is usual to define **P** as the diagonal matrix with the elements proportional to $k_r$. The population difference between the triplet sublevels ($\Delta P_\pm$) depends also on the relative orientation between the molecular frame and the magnetic field direction. This is given by [10]:

$$\Delta P_\pm(\Omega) = \pm \sum_{m=0,\pm 2} a_m D^2_{0m}(\Omega) \tag{7a}$$

where $D^2_{0m}$ are the second rank spherical harmonics, $\Omega = (\alpha, \beta, \gamma)$ the three Euler angles of the molecular frame with respect to the magnetic field direction and the $a_m$ are the irreducible spherical components of the matrix **P**.

If the motion is sufficiently fast (faster than the difference in frequency of the states involved) the angular dependence is averaged over the proper orientational distribution function. The population difference becomes:

$$\Delta P_{\pm} = \pm \sum_{m=0,\pm 2} a_m \overline{D^2_{0m}} \tag{7b}$$

where the upper bar over the spherical harmonics stands for the integration over $\Omega$. In this form the $\overline{D^2_{0m}}$ are the spherical components of the cartesian ordering matrix **S**. With some algebra the following expression is obtained:

$$\Delta P_{\pm} = \pm \mathrm{Tr}[\mathbf{S} \cdot \mathbf{P}] \tag{7c}$$

If **S** is known, the assignment of the principal values of the ZFS tensor to a particular molecular axis can be made by comparing the experimental spectra with those calculated on the basis of $D_{eff}$ and of the level population $P^{(nem)}$, expected from Eqs. (6) and (7).

## RESULTS

The TR-EPR spectrum of **1** recorded in the polycrystalline phase of E7 ($T = 130\,K$) 0.5 μs after the laser pulse is shown in Figure 1.

Only a very slight variation was observed by rotating the sample by 90°, showing that a negligible orientation in the solute is preserved in the freezing process. The spectrum is very similar to the spectra recorded for the same derivative and for other $C_{60}$ monoadducts in toluene isotropic frozen solution. The low field half of the spectrum is enhanced absorption and the high field one is in emission. The spectrum is simulated perfectly as an isotropic triplet powder spectrum [11] by assuming the ZFS parameters and triplet sublevels populations in the ratios reported in Table I. The sign of the ZFS parameters is not obtained from the simulation of TR-EPR spectra. It is assumed to be the same as for the pristine $C_{60}$ [12].

In the nematic phase, the TR-EPR spectrum of **1** recorded at a 0.5 μs delay after the laser pulse consists of two lines with opposite polarisation: at low field in emission and at high field in enhanced absorption (Fig. 2).

The spectral width is much smaller than that of the polycrystalline phase spectrum and the polarisation pattern is reversed with respect to that of Figure 1. Increasing the temperature in nematic range ($263\,K < T < 333\,K$) the line separation decreases (Fig. 3) and the intensity becomes smaller, until a weak single line is recorded in isotropic phase (Fig. 2).

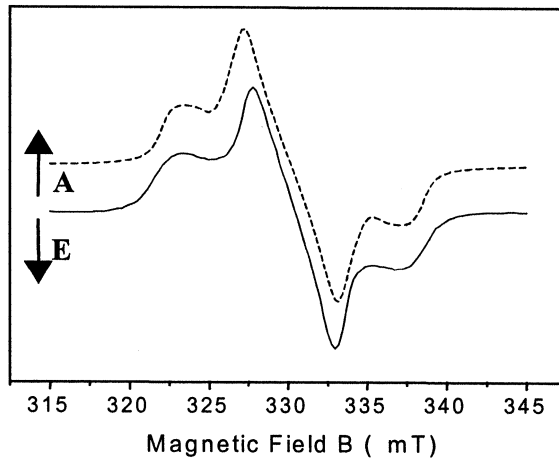


**FIGURE 1** TR-EPR spectrum of **1** in frozen polycrystalline phase (T = 130 K). Solid line: experimental spectrum, broken line: computed spectrum. The latter is vertically shifted for reasons of clarity. (A = absorption, E = emission).

The weak satellite lines appearing at a wider spectral width will be discussed below.

## DISCUSSION

Very recently we studied the EPR spectra of nitroxide $C_{60}$ adduct **2** in the nematic phase of PAA [13]. The g factor and the $^{14}N$ hyperfine splitting constant changed remarkably on going from the isotropic to the nematic phase. The variation was quantitatively accounted for by a preferential orientation along the liquid crystal director of the molecular axis *a*, which goes from the centre of the fullerene cage to the NO group. The other two perpendicular axes are indicated by *b* and *c*. The ordering matrix elements for the *a*, *b* and *c* axes ($S_{aa}$, $S_{bb}$, $S_{cc}$) were obtained from the variation of

**TABLE I** Triplet Zero Field Splitting Parameters and Sublevel Populations Used in the Simulation of TR-EPR of **1** in Frozen Polycrystalline E7 at 130 K

| Direction | Zero field splitting (gauss) | Relative zero field populations |
|---|---|---|
| X | −35 | 0.30 |
| Y | −20 | 1.00 |
| Z | +55 | 0.01 |

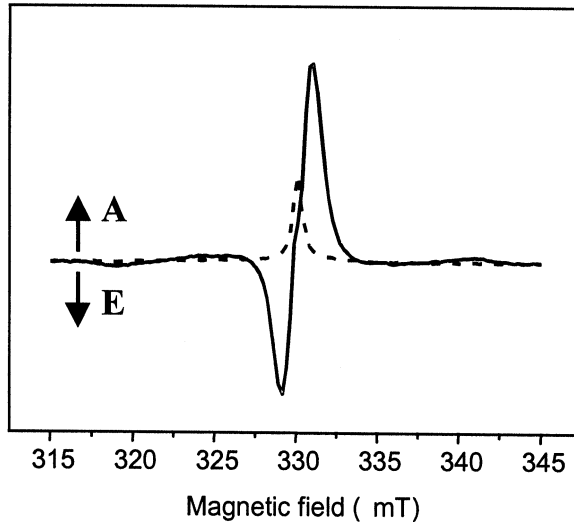


**FIGURE 2** TR-EPR spectra of photoexcited triplet state of **1** in nematic phase (T = 300 K, solid line) and in isotropic phase (T = 340 K, broken line) of E7. (A = Absorption, E = emission).

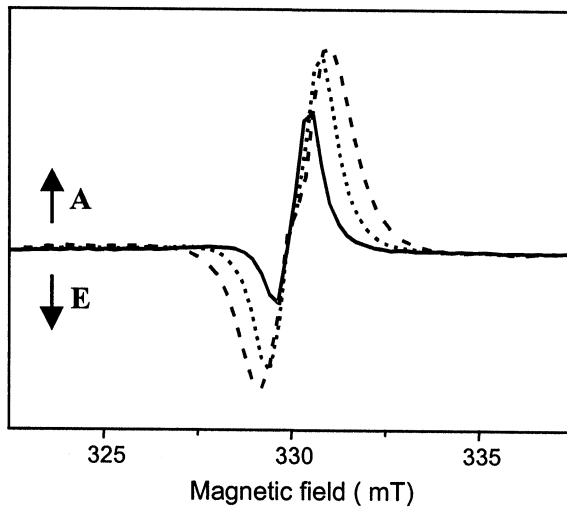


**FIGURE 3** TR-EPR spectra of photoexcited triplet state of **1** in nematic phase (T = 300 K broken line, T = 310 K dotted line, T = 320 K solid line) of E7. (A = absorption, E = emission).

the $^{14}N$ hyperfine coupling constant and of the g factor with respect to their values in the isotropic phase.

In this work we observed similar variations of the radical magnetic parameters when E7 was used as solvent. These variations are accounted for by the ordering matrix reported in Table II, which is very similar to that obtained for PAA at the same reduced temperature ($T/T_{NI} = 0.95$).

The ordering matrix **S** is in perfect agreement with that calculated on the basis of a model based on short range solute-solvent interactions [14]. This model predicts very marginal variations if the oxygen atom is replaced by an hydrogen one. Therefore, we may safely assume that **S** measured for the radical **2** holds also for the triplet state of **1**.

For the photoexcited triplet state of **1** in nematic E7, the effective dipolar interaction tensors and populations could be obtained from Eqs. (6) and (7), using the ZFS parameters D and E taken from the spectrum of the polycrystalline sample and the ordering matrix **S** from Table II. Since the *a* molecular axis (which is the axis of preferential orientation of the molecule) coincides with a symmetry axis, it should be a principal axis of the **D** tensor. There are three different choices: *a* is parallel respectively to X, Y or Z principal axes of electron dipolar interaction. Only the spectrum calculated for X parallel to *a* agrees with the experimental one, in particular it is the only one having the correct line separation and polarisation pattern. In order to illustrate this point we have drawn in Figure 4 the triplet energy level schemes in three different situations. They refer to the cases where one the principal axes X, Y and Z is preferentially oriented along the magnetic field direction and there is fast exchange of the other two axes, producing an averaging of energies and populations. It must be noted that the nematic director is parallel to the magnetic field, therefore the three schemes correspond to the *a* axis parallel to the principal directions. The EPR transitions and the substate populations are also shown and the resulting EPR spectrum is schematically drawn in the lower schemes of Figure 4.

Thus, we concluded that the X principal axis of the triplet state of $C_{60}$ monoadduct is directed along the *a* axis, which is the $C_2$ symmetry axis of the molecule. No information is allowed on the direction of the other axes Y and Z that could be either in the pyrrolidine plane or perpendicular to it.

**TABLE II** Principal Values of the Ordering Matrix Obtained for Compound **2** in PAA at $T/T_{NI} = 0.95$

| $\mathbf{S_{aa}}$ | $\mathbf{S_{bb}}$ | $\mathbf{S_{cc}}$ |
|---|---|---|
| 0.38 | −0.22 | −0.16 |

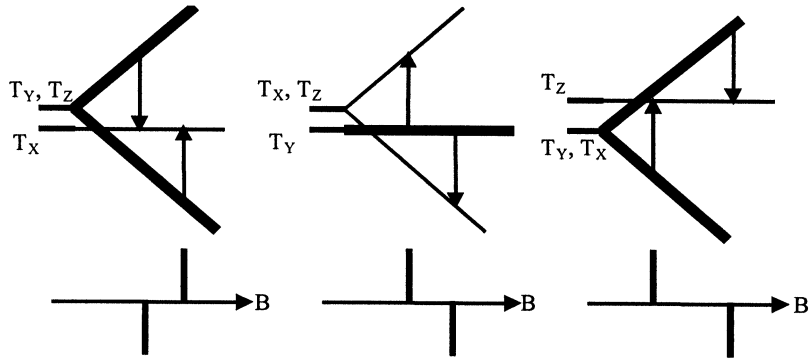


**FIGURE 4** Magnetic field energy level dependence (upper scheme) and calculated EPR stick spectra (lower scheme) of photoexcited triplet state of **1** in nematic phase with B parallel to X, Y, Z principal axes. Line thickness is proportional to relative populations.

## Temperature Dependence of $D_{eff}$

The decreasing of the line splitting in the triplet TR-EPR spectra of **1** in the nematic phase of E7 by increasing the temperature is due to the temperature variation of the ordering matrix **S**: the higher the temperature the smaller the **S** matrix principal values. The values for **2** at various temperatures in nematic phase of E7 are reported in Figure 5, where $S_{aa}$, $S_{bb}$ and $S_{cc}$ values are plotted against the reduced temperature.

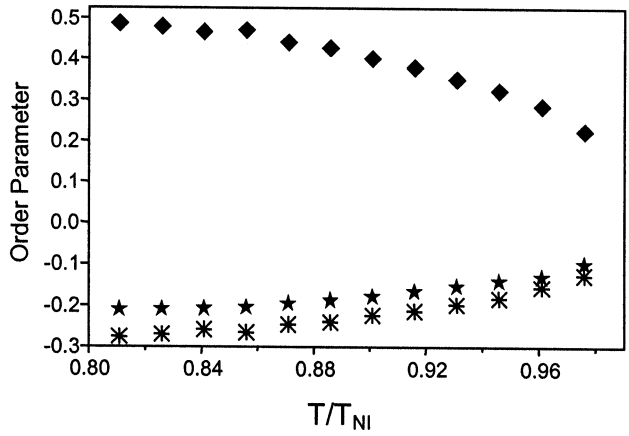


**FIGURE 5** Temperature dependence of the measured principal values ($S_{aa}$ diamonds, $S_{bb}$ stars and $S_{cc}$ asterisks) of the order matrix **S**.

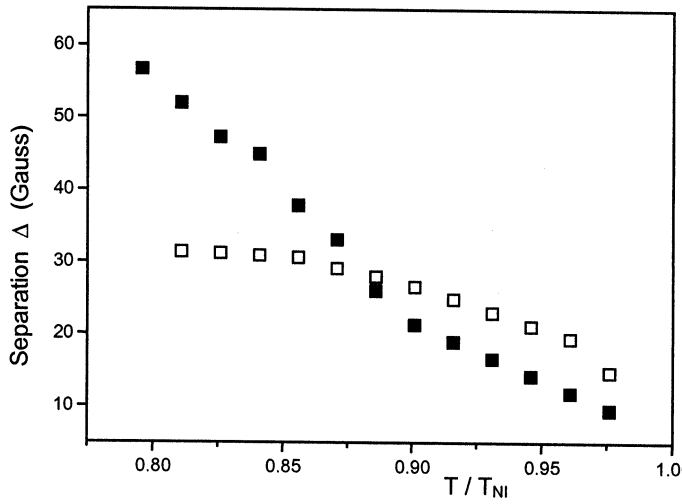


**FIGURE 6** Calculated values (empty square) and experimentally measured values (full square) of the splitting Δ of the EPR spectra of photoexcited triplet state of **1** in the nematic phase, at several reduced temperatures.

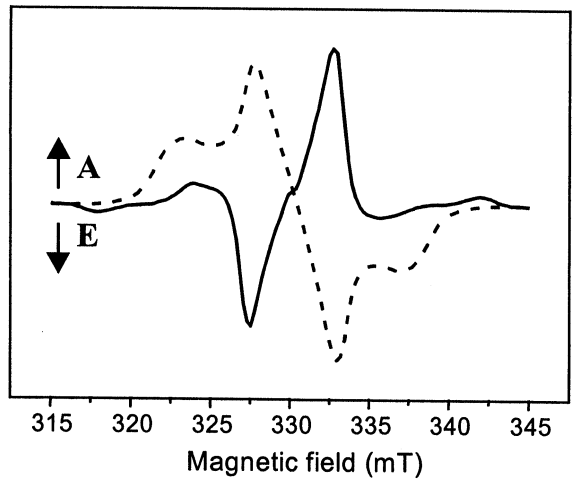


**FIGURE 7** TR-EPR spectra at 130 K (continuous line) and at 270 K (broken line) of photoexcited triplet state of **1**.

As in the previous discussion, we used these **S** values also for the triplet state of **1**, and calculated the $D_{eff}$ (Eq. 6) at several temperatures in the nematic range. The comparison with the experimental splitting is shown in Figure 6. The agreement is good at temperatures $T > 300\,K$

($T/T_{NI} = 0.90$) where the fast motion approximation, assumed in Eqs. (6) and (7), is valid.

At reduced temperatures lower than 0.90 (corresponding to $T < 300\,K$), the TR-EPR spectra become more complex and additional features emerge with a wider spectral width (Fig. 7). The splitting between the two central lines tends to the separation observed in the frozen solution. In these cases the lineshape analysis should be based on a slow motional regime model. We could get a reasonable simulation of the lineshape using a set of modified Bloch equations considering additional terms from exchange-like reorientation jumps. The calculated spectra reproduce the main features of the experimental ones even if the model is rather simplified. More sophisticated models could be devised, but this was beyond the scope of this work and was not pursued further.



## CONCLUSIONS

We studied the time resolved EPR (TR-EPR) spectra of the photoexcited triplet state of a fullerene $C_{60}$ monoadduct (Fulleropyrrolidine **1**) dissolved in E7 nematic solvent. In frozen polycrystalline phase of E7 the triplet state shows magnetic parameters (Zero Field Splitting and sublevel populations) very similar to other monoadducts in isotropic solvents. In nematic phase of E7 the TR-EPR spectra of the triplet state reduces to a doublet of polarised lines with Emission/Absorption phase. This lineshape can be interpreted in the frame of a fast motional regime of the $C_{60}$ derivative, with a preferential orientation. The direction of preferential orientation is parallel to the $C_2$ symmetry axis, approximately connecting the centre of the fullerene moiety and the nitrogen atom, as determined by the analysis of EPR spectra of the $C_{60}$ nitroxide adduct **2** dissolved in E7. The line separation and polarisation pattern of the triplet TR-EPR spectra of **1** can be reproduced only assuming that the X principal axis of the dipolar interaction is parallel to the $C_2$ axis. This represents a valuable information for the complete characterisation of the $C_{60}$ derivatives excited triplet states.

## REFERENCES

[1] Groenen, E. J. J., Poluektov, O. G., Matsushita, M., Schmidt, J., & van der Waals, J. H. (1992). *Chem. Phys. Lett.*, *197*, 314.

[2] (a) Bennati, M., Grupp, A., & Mehring, M. (1995). *J. Chem. Phys.*, *102*, 9457–9464. (b) Regev, A., Gamliel, D., Meiklyar, V., Michaeli, S., & Levanon, H. (1993). *J. Phys. Chem.*, *97*, 3671–3679.

[3] Agostini, G., Corvaja, C., Maggini, M., Pasimeni, L., & Prato, M. (1996). *J. Phys. Chem.*, *100*, 13416–13420.

[4] Kallày, M., Németh, K., & Surjan, P. R. (1998). ***J. Phys. Chem. A***, ***102***, 1261–1273.
[5] Zhang, D., Norris, J. R., Krusic, P. J., Wasserman, E., Chen, C. C., & Lieber, C. M. (1993). ***J. Phys. Chem.***, ***97***, 5886.
[6] Schick, G., Levitus, M., Kvetko, L., Brent, A. J., Lamparth, I., Lunkwitz, R., Ma, B., Khan, S. I., Garcia-Garibai, M. A., & Rubin, Y. (1999). ***J. Am. Chem. Soc.***, ***121***, 3246.
[7] Bingel, C. (1993). ***Chem. Berichte***, ***126***, 1957–1959.
[8] Mizuochi, N., Ohba, Y., & Yamauchi, S. (1999). ***J. Chem. Phys.***, ***111***, 3479–3487.
[9] Nordio, P. L. & Segre, U. (1979). In: ***The Molecular Physics of Liquid Crystal***, Lukhurst, G. R. & Gray, G. W. (Eds.), Academic Press: London, Chp. 16, 367–384.
[10] Gamliel, D. & Levanon, H. (1995). ***Stochastic Processes in Magnetic Resonance***, World Scientific: Singapore, 223–228.
[11] Segre, U., Pasimeni, L., & Ruzzi, M. (2000). ***Spectrochim. Acta, Part A***, ***56***, 265–271.
[12] van den Berg, G. J. B., van den Heuvel, D. J., Poluetktov, O. J., Hollemann, I., Meijer, G., & Groenen, E. J. J. (1998). ***J. Magn. Reson.***, ***131***, 39–45.
[13] Mazzoni, M., Franco, L., Ferrarini, A., Corvaja, C., Zordan, G., Scorrano, G., & Maggini, M. (2002). ***Liq. Cryst.***, ***29***, 203–208.
[14] (a) Ferrarini, A., Moro, G. J., Nordio, P. L. (2001). In: ***Physical Properties of Liquid Crystal: Nematics***, Dunmur, D. A., Fukuda, A., & Luckhurst, G. R. (Eds.), INSPEC: London, Chp. 2.3, 103–112.
(b) Ferrarini, A. & Moro, G. J. (2001). ***J. Chem. Phys.***, ***114***, 596–608.